Proceedings of the 8th International Conference on Structural Dynamics, EURODYN 2011
Leuven, Belgium, 4-6 July 2011
G. De Roeck, G. Degrande, G. Lombaert, G. Müller (eds.)
ISBN 978-90-760-1931-4

Vibration emission induced by Rapid Impact Compaction

Dietmar Adam[1], Christoph Adam[2], Franz-Josef Falkner[2], Ivan Paulmichl[3]
[1]Department of Civil Engineering, Vienna University of Technology, Karlsplatz 13, 1040 Vienna, Austria
[2]Department of Civil Engineering Sciences, University of Innsbruck, Technikerstr. 13, 6020 Innsbruck, Austria
[3]Geotechnik Adam ZT GmbH, Wiener Str. 66-72/15/4, 2345 Brunn am Gebirge, Austria
email: d.adam@tuwien.ac.at, christoph.adam@uibk.ac.at, franz.falkner@uibk.ac.at, paulmichl@geotechnik-adam.at

ABSTRACT: This paper presents results of experimental and numerical studies concerning the dynamic effects of the Rapid Impact Compactor (RIC) on its environment. The RIC is a dynamic compaction device for middle-deep ground improvement based on the piling hammer technology used to increase the bearing capacity of soils through controlled impacts. The procedure of the assessment of the damage potential of RIC on adjacent buildings, buried pipes, etc., which must be performed reliably in advance, is described in detail. The results of experimental investigations on the vibrations induced by the RIC demonstrate the successful application of the innovative compaction method in built-up area. This conclusion is supported by the outcomes of numerical simulations.

KEY WORDS: Rapid Impact Compaction; Vibration emission/immission; Vibration monitoring; Wave propagation.

1 INTRODUCTION

1.1 Motivation for this study

Proper load transfer of building loads into the underground requires foundation on subsoil, which exhibits low settlements and sufficient load-bearing capacity. Thus, compaction of soil with insufficient ground bedding condition is of particular significance. Appropriate compaction increases the soil density, which in turn give rise to homogenized subsoil, reduced settlement and enhanced load-bearing capacity. The serviceability and the structural safety of the complete building connected to the earth structure are ensured and damage is prevented.

Numerous developments of the last decades provide a broad range of near-surface compaction technologies (such as static and dynamic rollers) and deep compaction techniques (such as deep vibro-compaction, vibro-flotation and deep vibro-replacement, heavy tamping). However, until recently no device was available for middle-deep compaction. The lately introduced Rapid Impact Compactor (RIC) aims at closing the gap between the surface compaction methods and the deep compaction methods, and permitting a middle-deep improvement of the ground up to a depth of 4 to 7 m [1].

For the assessment of the damage potential of the RIC on adjacent buildings, buried pipes, etc., the vibration emission must be evaluated reliably in advance. Since the RIC is a relatively novel device a comprehensive study was initiated to gain knowledge about its dynamic effect on the environment and its efficiency.

1.2 The Rapid Impact Compactor and its application

The RIC is an innovative dynamic compaction device based on the piling hammer technology and is used to increase the load-bearing capacity of soils through controlled impacts. The general idea of this method is to drop a falling weight from a relatively low height onto a special foot assembly at a fast rate while the foot remains permanently in contact with the ground [2].

Figure 1. Rapid Impact Compactor (left), impact foot with driving cap (center top), points of compaction (center bottom), and compaction process (right).

The RIC consists mainly of three impact components: the impact foot, the driving cap, and the hammer with the falling weight. The impact foot made of steel has a diameter of 1.5 m. Since the driving cap is connected loosely to the foot, only compression forces load the subsoil, which allows an efficient energy transfer. Impact foot, driving cap, and falling weight are connected to the so-called hammer rig (see Figure 1). Falling weights of mass 5,000, 7,000, 9,000 or 12,000 kg are dropped from a falling height up to 1.2 m at a rate 40 to 60 repetitions per minute [1]. For further details see [3].

Gravels, sands, silts, industrial byproducts, tailings material, and landfills can be successfully compacted by the RIC to increase the load-bearing capacity of foundations, to improve the ground bedding conditions for slabs, to reduce the liquefaction potential of soils, and to stabilize waste materials.

1.3 Objective

In the first part of this study characteristic parameters for the assessment of vibration induced structural and non-structural damage with emphasis to RIC applications are identified. Furthermore, standards and regulations with respect to vibration immission on buildings are evaluated. It is noted that

emphasis is on regulations that are effective in Austria and Germany.

Theoretical investigations comprise numerical computer simulations of the wave propagation induced by the RIC. In an engineering-like approach for the subsoil the material properties of silty fine sand, loose sandy gravels, and dense gravels are employed assuming rate-independent plasticity. Experimental tests on different soil conditions provide the verification of theoretical analyses.

Table 1. Building parameters and their impact on the dynamic structural parameters.

Building parameter		**Impact on dynamic structural parameter**
Dimension:	Building dimension and number of floors	Natural frequencies of the structure
Foundation:	Strip foundation, foundation slab, deep foundation	Damping
Structural system:	Brick/concrete structure, structure of pre-fabricated segments, steel frame supporting structure, timber structure	Vibration behaviour
Slab structure:	Timber/lightweight structure, pre-fabricated segments or concrete structure, and span width	Natural frequencies of the slab, vibration behaviour
Construction history:	Construction year, rebuilding, damages due to war, etc.	Stability

2 ASSESSMENT OF THE DAMAGE POTENTIAL OF RAPID IMPACT COMPACTION

2.1 Fundamentals

Vibration can be defined as more or less regularly repeated movement of a physical object about a fixed point. A number of sources may generate ground-borne vibrations, including moving vehicles on road and railways, construction activities such as dynamic compaction piling, blasting, and tunnelling.

Vibrations propagate in the ground from the vibration source to an adjacent building, buried pipes, etc., predominantly through energy-rich surface waves, which are referred to as Rayleigh waves [4]. Less important for excitation of surface or near-surface structures is the energy transport through body waves in the subsoil. Body waves can be distinguished between compression waves (P-waves) and shear waves (S-waves) [4]. The amplitude of these waves decreases with increasing distance from the source. This attenuation can be attributed to the expansion of the wave front, which is referred to as geometrical damping [5], and secondly to the dissipation of energy within the soil itself. The latter is generally known as material damping. The rate of geometrical attenuation depends on the type of wave and on the shape of the corresponding wave front. Material damping is generally defined as energy loss due to hysteresis depending on many parameters such as soil type, moisture content, and temperature. In addition, material damping is a function of the vibration amplitude.

Structural vibrations may result in building damage, and may affect vibration-sensitive equipment inside of buildings. People may be disturbed or annoyed or, at higher levels, vibration even affects a person's ability to work [6].

The compaction effect of the Rapid Impact Compactor is characterized by pulse-shaped loading of the ground and is achieved by a specific number of blows. The ground to be improved is both compacted and displaced depending on the soil type, thus, causing plastic deformations in the near-field while elastic waves are generated in the far-field. The nature of vibration excitation (transient or periodic) is one of the limiting factors for the allowable impact on buildings and human beings and has to be taken into account for the assessment of standardized limit values.

Dynamic parameters, which affect the impact of vibrations on protected properties such as buildings, technical equipment, and machinery inside of buildings, as well as significant parameters for vibration recording and evaluation are described in the following. Note that vibration immission on human beings inside of buildings is not discussed.

2.2 Vibration immission on structures

Mechanical vibrations depend both on the excitation characteristics and on the properties of the excited building. The excitation is primarily characterized by its intensity, duration, time history, and frequency content. For a building the type of structure, material properties, construction quality, natural frequencies, and inherent damping, amongst others, have a severe impact on its dynamic response.

According to several international standards, such as the Austrian standard ÖNORM S 9020 [7] and the German Standard DIN 4150-3 [8], the peak particle velocity of the foundation correlates best with monitored building damages in the relevant intensity spectrum and frequency spectrum. The velocity is measured in three orthogonal directions denoted by x, y, and z. The square root of the sum of the squares of the corresponding velocity components v_x, v_y and v_z is denoted as velocity magnitude v_R. Its maximum during a single event, the peak velocity magnitude $v_{R,\max}$,

$$v_{R,\max} = \sqrt{v_x^2(t) + v_y^2(t) + v_z^2(t)}\Big|_{\max} \tag{1}$$

expressed in millimetres per second (mm/s), is the characteristic response parameter for the assessment of the damage potential of ground motions on adjacent structures.

The upfront estimation of the dynamic behaviour of a building requires the evaluation of the following parameters (see Table 1):

- Size of the building
- Age of the building
- Structural system
- Foundation
- Number of floors
- Slab structure

Thereby, the structural system, which includes layout, structural material, stiffening elements, etc., is the most significant parameter. Consequently, the Austrian Standard ÖNORM S 9020 [7] distinguishes between four building classes I to IV with respect to the structural system, as shown in Table 2. For each class an allowable value $v_{R,\max}$, monitored

at the foundation, is defined. In the second column of Table 3 upper limit values of $v_{R,\max}$ according to the Standard ÖNORM S 9020 [7] are specified, which are applicable as guide values for vibrations induced by infrequent singular blasting and comparable pulse-shaped immissions induced by the RIC. If the actual values are smaller than these regulated values, the dynamic building load can generally be assumed as allowable.

According to [7] for frequent immissions (once or several times a day) the values given in the second column of Table 3 must be reduced by 20%. The corresponding values are specified in column 3. Long-lasting temporary vibrations induced by demolition work, drilling, piling, and dynamic compaction work have to be monitored with respect to building damage. Experience has proven that a reduction to 40% of the values specified in [7] can be employed as guide value on-site, see Table 3, column 4. Contrary, in the German standard DIN 4150-3 [8] and in the Swiss standard SN 640 312 a [9] the allowable values are defined in dependence of the frequency.

Table 2. Building classes according to the Austrian Standard ÖNORM S 9020 [7].

Buildung class	Structure
I	Industrial structures - Frame structures (with or without core) of steel and/or reinforced concrete - Wall structures (concrete, pre-fabricated segments) - Engineering timber structures (e.g. halls)
II	Residential buildings - Frame structures (like I) - Wall structures (like I) - Structures with concrete slabs, walls made of concrete, brick, masonry with cement or lime mortar - Timber structures, except half-timbered buildings
III	Frame structures with less strength than structures of class I and II: Structures with basement slabs of concrete or brick arches and pre-fabricated parts, timber beam or pre-fabricated brick slabs in the upper floors Brick lined half-timbered buildings
IV	Listed buildings particularly sensitive to vibrations

Table 3. Reference values for the allowable peak velocity magnitude $v_{R,\max}$ [mm/s] (measured at the foundation) according to the Austrian Standard ÖNORM S 9020 [7].

Building class	Allowable peak velocity magnitude max $v_{R,\max}$ [mm/s]		
	Infrequent blasting (weekly)[1]	Frequent blasting (daily)[2]	Long-lasting temporary vibrations[3]
I	30	24	12
II	20	16	8
III	10	8	4
IV	5	4	2

[1] according to ÖN S 9020, Table 3
[2] values acc. to ÖN S 9020, Table 3, reduced by 20% according to ÖN S 9020
[3] values acc. to ÖN S 9020, Table 3, reduced by 60% according to experience

Vibrations are monitored at the point of the building foundation closest to the vibration source. If construction work takes place simultaneously at different places more than one monitoring location may be required. In some situations access to a building vulnerable to vibrations is not possible. Then, locations may be at or just within the site boundary. It is noted that according to ÖNORM S 9020 [7] measurements in the free-field cannot be used for a standardized estimation of vibration immissions on buildings.

The Austrian Standard ÖNORM S 9010 [10] discusses the measurement of vibration in buildings in general terms. More specific advice for damage investigation is given in the Austrian Standard ÖNORM S 9020 [7].

Table 4. Sensitivity classes of technical equipment.

Sensitivity class	Machine, instrument
I	Facilities for dressing optical devices to size and calibrate precision scales; microscopes; interferometer; optical precision devices; mechanical measurement and control devices up to tolerances in the order of a few 1/1000 mm; etc.
II	Ball bearing, cogwheel and thread grinding machines; automatic grinding machines; precision milling machines and lathes up to tolerances in the order of a few 1/100; automatic units for grinding razor blades etc.
III	Metal working lathes, milling, boring, grinding machines and other metal working machines of common class of accuracy; spinning and weaving machines; printing press machines; sewing machines
IV	Ventilators, centrifuges, electric motors, puncher and squeezing machines in metal working and light industries, piston drills, vibrators, vibrating tables, vibrating sieves, spreaders etc.

2.3 Vibration immission on vibration-sensitive technical facilities in buildings

Precision equipment vulnerable to vibration immissions is utilized in many industries including fabrication and manufacturing of microchips, other electronic equipment, particle or laser beams for magnification and measurement, and medical equipment such as magnetic resonance imaging (MRI) machines. The required precision of this type of equipment is in the range of micrometers (10^{-6} m) to picometers (10^{-12} m). Slightest vibrations or movements lead to an exceedance of the tolerance range and thus to defective outcomes. Financially costly disruption, in terms of a manufacturing or fabrication plant, or a time expensive disruption, in terms of research, may be the result. If the out-of-tolerance movement is not noticed, inaccurate images or measurements are obtained.

Vibration immissions on vibration-sensitive machinery and equipment can generally yield the following problems:

- Production process (e.g. tolerance or precision problems)
- Impairment of operational reliability (e.g. balance, medical equipment such as MRI)
- Impairment of serviceability (e.g. incompatible deformations, fatigue problems)

The guide values defined in the Austrian and German Standards ÖNORM S 9020 [7] and DIN 4150-3 [8],

respectively, are not applicable to vibration-sensitive technical facilities. No generally valid limit values can be specified, because allowable vibration immissions depend strongly on the machine specification. Thus, machine manufacturers provide guidelines of allowable vibration immission such as peak acceleration or peak velocity magnitude with respect to the excitation frequency in form of limit curves.

In Table 4 four sensitivity classes for machines and instruments are distinguished. A more general assignment of frequency dependent guide values in dependence of the sensitivity class is given in Table 5. Guide values for allowable velocity immission on vibration-sensitive computer facilities depend on the dominant frequency and are typically between of 0.2 and 2.0 mm/s.

According to the German Standard DIN 4150-3 [8] the values of Table 6 must be reduced by 50% when utilized for permanent vibrations.

Table 5. Guide values for vibration immissions on machines with respect to the sensitivity class according to Table 4

Sensitivity class	Sensitivity against harmonic vibrations	Allowable amplitude	
		Peak acceleration [mm/s^2]	Peak velocity [mm/s]
		1 – 10 Hz	10 – 100 Hz
I	High	6.3	0.1
II	Moderate	63	1
III	Low	250	4
IV	Insensitive	> 250	> 4

Table 6. Guide values for the peak velocity components $v_{i,\max}$ ($i = x, y, z$) measured on buried pipes according to the German Standard DIN 4150-3 [8].

Pipe class	Pipe material	$v_{i,\max}$ [mm/s]
1	Steel, welded	100
2	Vitrified clay, concrete, reinforced concrete, prestressed concrete, metal	80
3	Bricking, synthetic material	50

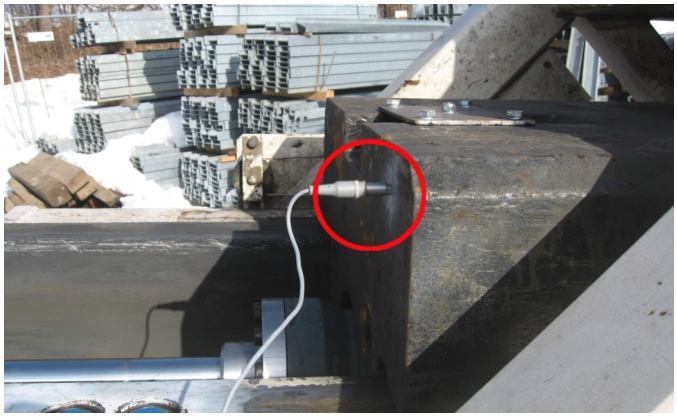

Figure 2. Acceleration sensor mounted on the falling weight of 9,000 kg.

Figure 3. Acceleration sensor mounted on the compaction foot.

Figure 4. Measurment chain and acceleration sensor mounted in the near-field of the compaction foot (right).

2.4 Vibration immission on buried pipes

The German Standard DIN 4150-3 [8] defines guide values for the estimation of the impact of short-time vibrations on buried pipes. The application of the standardized values given in Table 6 requires the installation of the pipes according the current state of the art. It is noted that for pipes in a distance less than 2 m from a building the guide values for buildings must be utilized.

3 EXPERIMENTAL STUDY OF VIBRATIONS INDUCED BY THE RAPID IMPACT COMPACTOR

Subsequently, results of experimental tests are presented aiming at revealing the damage potential of the RIC at adjacent buildings and equipment vulnerable to vibrations. Large-scale tests on various test tracks and different ground conditions have been performed. For these experimental investigations dynamic gauges were installed both in the ground and on the compaction device in order to measure the vibration behaviour of the complete device-underground interaction system. The outcomes serve as reference for verifying the results of a comparative numerical study.

3.1 Vibration source

The acceleration of the impact foot of the RIC can be considered as emission source of vibrations induced by the RIC. Thus, in an initial test the acceleration of the falling

weight and of the impact foot was measured. The measurements were conducted during a test compaction at the property of the Austrian company TERRA-MIX [11]. In this test a falling weight of 9,000 kg was employed. The subsoil to be compacted consisted of stiff silts (loam) covered by anthropogenic fillings (brick) with a layer thickness of 0.5 to 0.75 m. Inductive acceleration sensors of the type B12 (HBM Hottinger Baldwin Messtechnik [12]) connected to a HBM measuring amplifier DMCplus were employed. The measured data were recorded and evaluated on a notebook with the software Catman [12]. Figure 2 and Figure 3 show the position of the accelerations sensors on the falling weight and the compaction foot, respectively. In addition, an acceleration sensor was installed at a distance of about 5 metres from the compaction centre, as depicted in Figure 4.

As selected result of the measurements Figure 5 shows the time histories of the vertical acceleration components of the falling weight, the impact foot, and the subsoil surface at 5 metres distance. It can be seen that the compaction foot exhibits a vertical peak acceleration of 386 m/s^2 instantaneously after the falling weight hits the driving cap. In comparison, the vertical peak acceleration of the impact foot is about 56 m/s^2, and of the subsoil about 45 m/s^2.

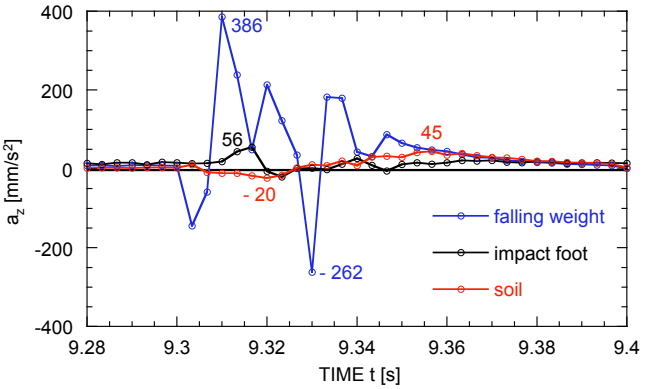

Figure 5. Vertical acceleration component of the falling weight, impact foot, and soil surface induced by one blow of the RIC. Falling mass: 9,000 kg. Recorded data.

3.2 *Vibration emission*

On various free-field test sites the peak soil surface velocity magnitude with respect to the distance from the compaction foot was determined. Note that in a free-field no structures with significant mass are close to the compaction point. The data acquisition tool MR2002DIN-CE (RED BOX) of company SYSCOM was applied to monitor and record this vibration quantity. The velocities were measured in situ with tri-axial velocity transducers of the company SYSCOM [13] (type MS2003 A3HV 315/1) according to the German Standard DIN 45669-1 [14] in combination with a data recorder (SYSCOM, type MR2002 DIN-CE). During the Rapid Impact Compaction the velocity was measured in three orthogonal directions in the frequency domain of 1 to 315 Hz. The subsequent data processing was conducted with the software package VIEW 2002 [15]. Subsequent regression analyses of the measured peak velocity magnitudes $v_{R,\max}$ at discrete surface points rendered $v_{R,\max}$ as function of the distance from the impact foot.

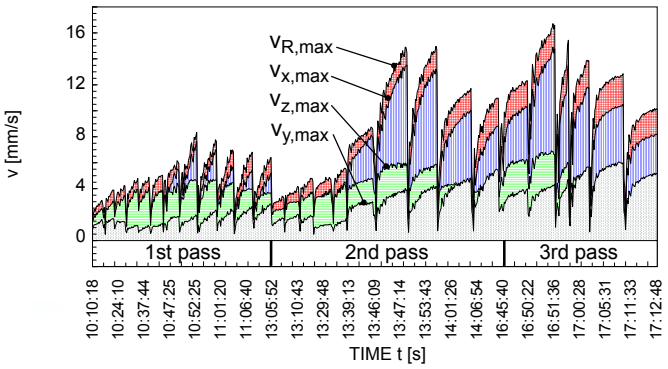

Figure 6. Magnitude of the peak velocity components $v_{x,\max}$, $v_{y,\max}$, $v_{z,\max}$ and peak velocity magnitude $v_{R,\max}$ measured during Rapid Impact Compaction.

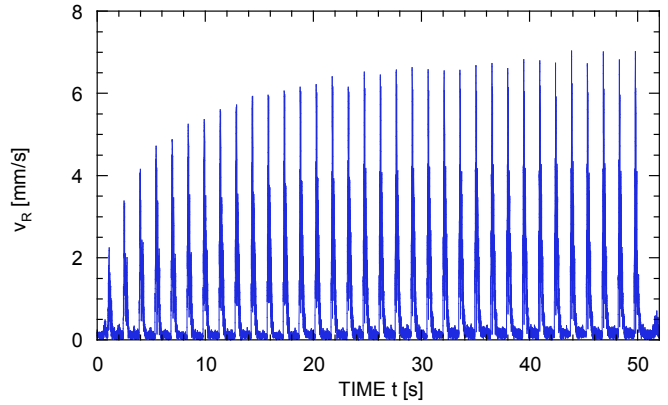

Figure 7. Velocity magnitude v_R at a selected surface point. RIC with a falling weight of 9,000 kg. Measured data.

In a fundamental test it was studied whether the RIC can be employed for improving the impermeability of existing dams. Thus, in Fischamend, Austria, a test dam was built with well-defined boundary conditions. In the course of the experiment the core of the dam composed of loam and clay was compacted by the RIC. For details of the test set-up, subsoil conditions, and work-flow see [3]. The applied compaction process comprised three passes. I.e. each compaction point was compacted with three series of successive compaction blows. Between each pass the soil was at rest.

As a result Figure 6 represents the peak velocity magnitude $v_{R,\max}$ and the corresponding peak velocity components $v_{x,\max}$, $v_{y,\max}$, $v_{z,\max}$ in orthogonal directions x (horizontal), y (horizontal), z (vertical), respectively, at a selected surface point with a distance of 11.5 to 15 m from the individual compaction points. Each "saw tooth" of this figure represents the peak velocities during the compaction process (of 30 to 60 hits) at one compaction point of the test field. It can be seen that the peak velocities are larger the closer the actual compaction point to the monitoring location. The horizontal component $v_{x,\max}$ dominates the particle velocity. Furthermore, the peak velocity magnitude increases with each successive blow applied at the same compaction point. This fact can be observed considering each "saw tooth" separately, and is supported by Figure 7. In Figure 7 the time history of the velocity magnitude during a single compaction pass, which

comprises 33 blows, is depicted. It is readily observed that with each blow the peak velocity magnitude increases. However, with increasing soil compaction the gradient of this increase becomes smaller until it stays more or less constant.

Compaction tests on various subsoil conditions in the free-field reveal that the peak velocity magnitude decreases in a double-logarithmic representation more or less linear with increasing distance from the compaction foot. Figure 8 shows selected linear regression lines for different homogeneous ground conditions determined through free-field velocity measurements during RIC compaction with a falling weight of 9,000 kg. It is seen that smallest peak velocity magnitudes develop during compaction of homogeneous loose sandy gravels. For this subsoil condition a coefficient of decay of about 1.8 is determined. Note that only one compaction pass was performed. Largest peak velocity magnitudes were measured during compaction of dense gravels. Compaction of sandy silts and gravelly silty sands led to peak velocity magnitudes in-between. The coefficient of decay of about 1.3 is practically identical for dense gravels, sandy silts, and gravelly silty sands. The results show that the peak velocity magnitude falls below the value of max $v_{R,\max}$ = 10 mm/s at a distance of 11 to 34 m from the impact foot, depending on the subsoil condition and soil type.

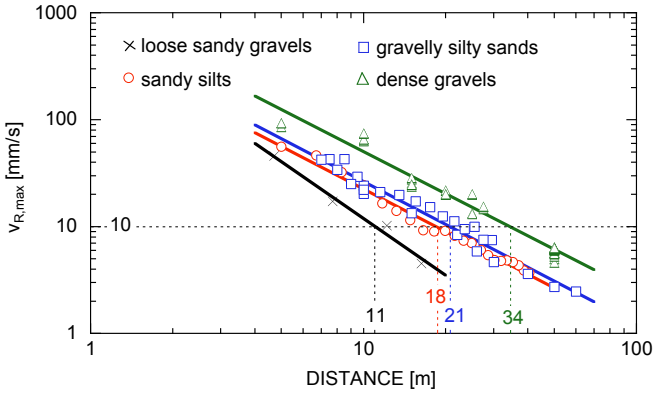

Figure 8. Peak velocity magnitude $v_{R,\max}$ as function of distance from the impact foot. RIC with a falling weight of 9,000 kg. Measured data.

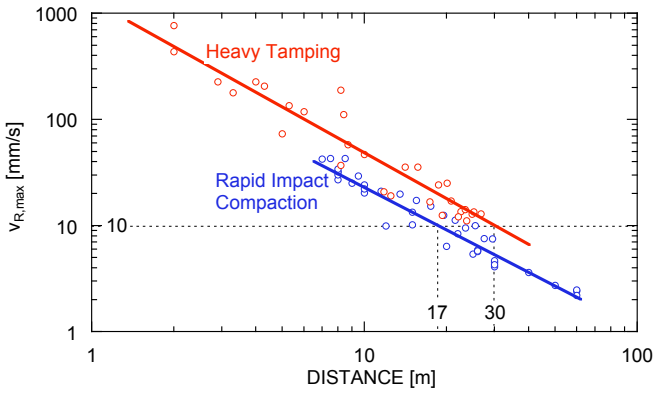

Figure 9. Peak velocity magnitude $v_{R,\max}$ as function of distance from the impact point. RIC induced (falling weight: 9,000 kg) and heavy tamping induced (falling weight: 16,500 kg) vibrations [1].

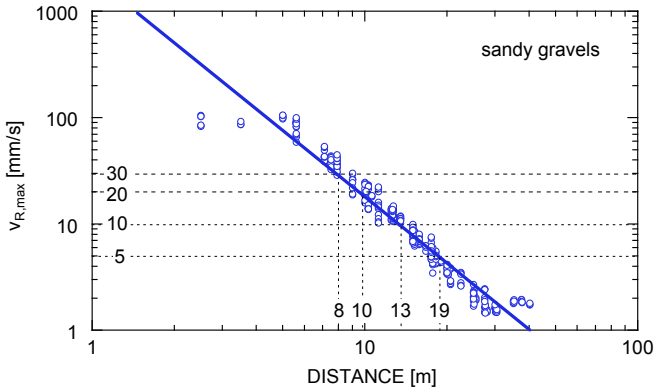

Figure 10. Peak velocity magnitude $v_{R,\max}$ as function of distance from the impact foot. RIC with a falling weight of 7,000 kg. Measured data.

In Figure 9 the vibration emission of heavy tamping and the RIC are set in contrast. Heavy tamping is a deep compaction method, where a falling weight of 16,500 kg is dropped from a height of 20 to 25 m to the subsoil. It can be seen that in the presented example heavy tamping induces peak velocity magnitudes of more than 10 mm/s at distances up to 30 m to the impact point, whereas for the RIC the limit distance to the impact foot for vibrations amplitudes of 10 mm/s is 17 m.

Measurements during RIC compaction of sandy gravels with a falling weight of 7,000 kg resulted in the velocity-distance relation visualized in Figure 10. In this particular example the peak velocity magnitude falls below the limit value of max $v_{R,\max}$ = 10 mm/s at a distance of about 13 m from the impact foot.

3.3 Vibration immission

In several tests subsoil compaction close to structures RIC induced vibrations were monitored inside of buildings, close to vibration sensible equipment located inside of buildings, and close to or above buried pipes utilizing the same data acquisition tool described before for free-field measurements. Thereby, the peak velocity components in three orthogonal directions, and the peak velocity magnitudes were recorded every 30 seconds. In addition, when the trigger value of $v_{R,\max}$ = 2 mm/s was exceeded, the corresponding peak response value was registered.

Exemplarily, the outcome of a RIC venture conducted in Trier, Germany, is presented. For the construction of a production hall man-made fill (silt, sand, gravel) below the foundation level was improved by the RIC adjacent to an existing hall of building class I according to the Austrian Standard ÖNORM S 9020 [7]. For such a structure the maximum allowable peak velocity magnitude is max $v_{R,\max}$ = 12 mm/s (compare with Table 3). At first the safety distance between the RIC and the existing hall was determined based on vibration measurements. Since the foundation of the existing building was inaccessible, the tri-axial velocity transducer was placed close to the external load-bearing wall at ground floor level. Measurements during the compaction on a test field have shown that the RIC can be applied up to a minimum distance of about 5 to 7.5 m from the existing structure in order to meet the allowable limit value of max $v_{R,\max}$ = 12 mm/s. Figure 11 shows the peak

velocity magnitudes at discrete instants, which were recorded during the compaction process. It can be seen that the observed maximum is about $v_{R,\max} = 10.7$ mm/s. Thus, the allowable limit value was met.

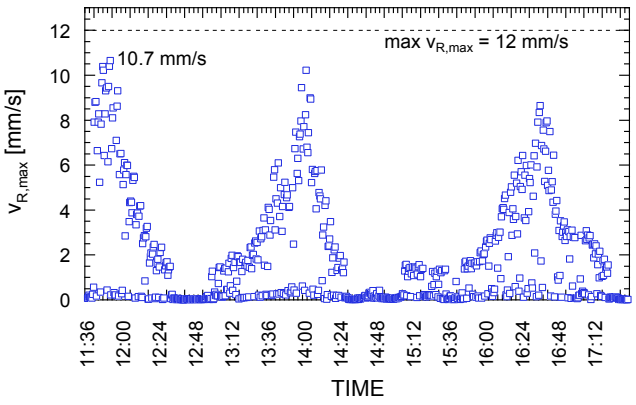

Figure 11. RIC induced peak velocity magnitude $v_{R,\max}$ recorded at a production hall. Falling weight: 9,000 kg. Measured data.

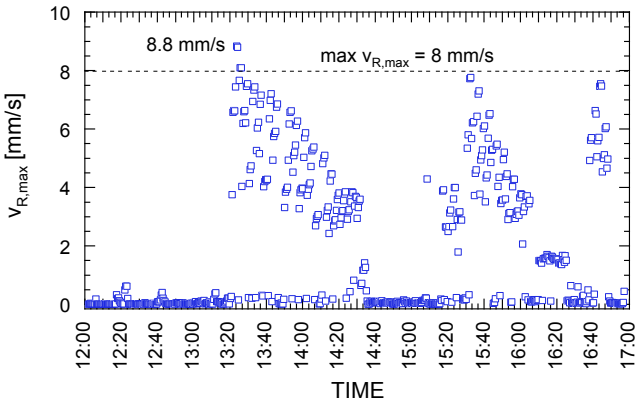

Figure 12. RIC induced peak velocity magnitude $v_{R,\max}$ recorded in residential neighbourhood. Falling weight: 9,000 kg. Measured data.

In a further example, RIC induced vibrations measured during the ground improvement for a structure to be built in a residential neighbourhood of building class III according to Table 2 and Table 3 in the City of Vienna, Austria, are discussed. Alluvial silts and sands resting on alluvial sandy gravels were stabilized with lime up to 0.5 m beneath excavation level and compacted with the RIC affecting the sandy gravels as well. Thereby, a tri-axial velocity transducer was placed close to the load-bearing external wall at ground floor level in a distance of about 15 m from the construction site. Figure 12 shows the recorded peak velocity magnitude as a function of time. The measurements resulted in a peak velocity magnitude of about 8.8 mm/s. Thus, the allowable limit value max $v_{R,\max} = 8$ mm/s (compare with Table 3) was exceeded in the order of about 10%. However, according to the Standard ÖNORM S 9020 [7] a sporadic exceedance up to 20% can be tolerated. This specification was validated, because no damage on the adjacent buildings could be observed.

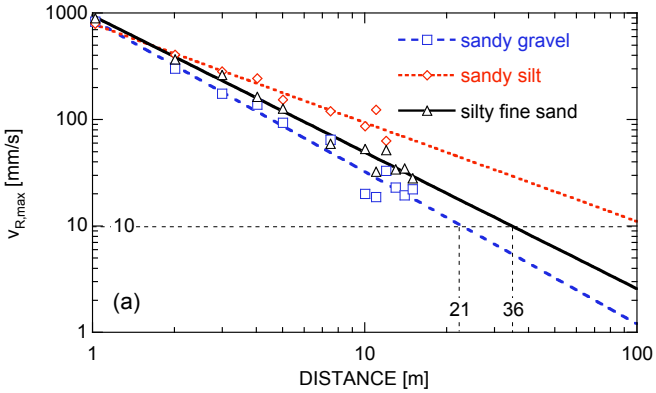

Figure 13. Peak velocity magnitude $v_{R,\max}$ as function of distance from the impact foot. Numerical outcomes.

4 THEORETICAL STUDY OF VIBRATIONS INDUCED BY THE RAPID IMPACT COMPACTOR

A theoretical study of the dynamic impact of the RIC on its environment was performed employing a simple mechanical model of the RIC-subsoil interaction system. Thereby, the falling weight is modelled as lumped mass, and hits the impact foot after a free fall. The initial velocity of the impact foot, which excites the underground, is derived assuming an idealized elastic impact between falling weight and the mass of the impact foot. The soil medium is modelled as homogenous, isotropic, and rate-independent elastoplastic halfspace based on Mohr-Coulomb theory with isotropic hardening. The axially symmetric impact foot made of steel rests on the surface of the halfspace. A sliding interface between the foot and the soil is adopted, i.e. only normal stresses are transferred between the foot and the soil. The numerical model takes advantage of the rotational symmetry of this subsystem, which is divided into a near-field and a far-field. The near-field is discretized by means of Finite Elements. Infinite Elements model the far-field in order to avoid wave reflections at the boundary between the near- and far-field, and to allow for energy propagation into the semi-infinite halfspace. The model and its parameters are described in more detail in [3].

As an example, Figure 13 shows the decay of magnitude of the numerically derived peak velocity magnitude $v_{R,\max}$ in the free-field as function of the distance from the compaction point. Sandy silt, silty fine sand, sandy gravel are the underlying soil conditions. The employed material parameters are listed in [3]. The maximum values of $v_{R,\max}$ at discrete surface points are plotted in logarithmic scale. It is illustrated that in such a representation a linear regression line approximates the decay of numerically derived vibration amplitudes, in the same manner as for the experimentally derived peak velocity magnitudes. The graphs of this figure demonstrate that the decay of vibrations with respect to the distance from the compaction point depends on the lateral contraction behaviour of the soil: The smaller the lateral contraction behaviour the faster the decay of vibrations. Possion's ratio of non-cohesive soils (sandy gravel) is smaller than for mixed grained soils (silty fine sand). Cohesive soils (sandy silt) exhibit the largest Poisson's ratio, because the moisture content of this type of soil is largest. Water is almost

incompressible, and thus, the decay of vibration is slow. This behavior has also been observed during various applications of the RIC on-site.

In Figure 14 the peak velocity magnitude $v_{R,\max}$ is shown with respect to the distance of the compaction point for the subsoil condition silty fine sand after the first, third, fifth, and tenth compaction pass. The outcomes of this figure prove field observations that the pronounced increase of $v_{R,\max}$ after each compaction impact leads to a parallel shift of the regression line, and thus, the arbitrary assumed limit value of 10 mm/s is shifted to a larger distance from the compaction point.

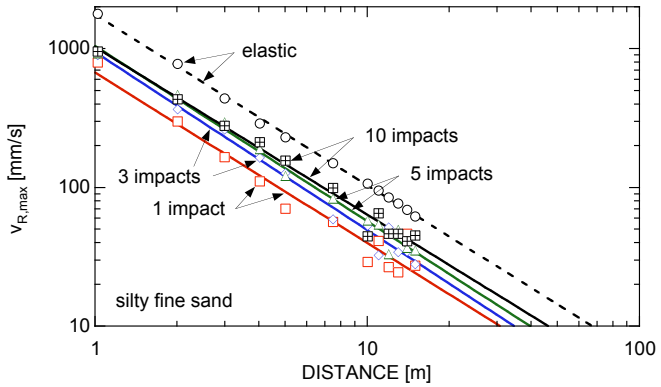

Figure 14. Peak velocity magnitude $v_{R,\max}$ as function of distance from the impact foot. Numerical outcomes.

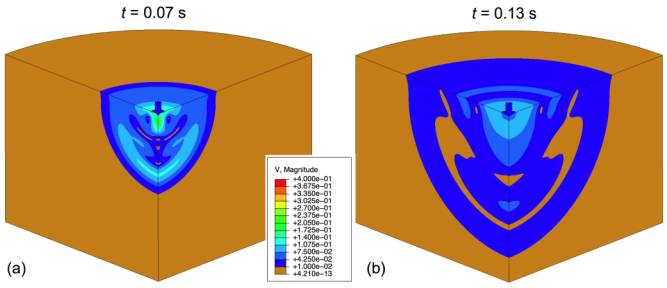

Figure 15. Distribution of the velocity magnitude at two specified instants after the first compaction impact. Elastoplastic silty fine sand.

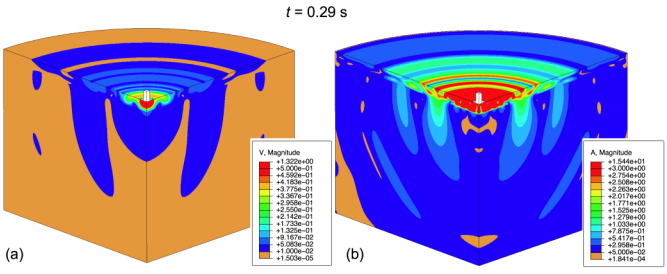

Figure 16. Distribution of the velocity (left) and acceleration (right) magnitude at one specified instant after the first compaction impact. Elastoplastic silty fine sand.

Subsequently, the spatial wave propagation induced by Rapid Impact Compaction is discussed based on numerically derived results. Figure 15 shows the propagation of the velocity magnitude at two instants after the first impact is applied to the subsoil with assigned parameters of elastoplastic silty fine sand. A cross-section below the impact point of the complete near-field, which is discretized by means of Finite Elements, is depicted. Spherical propagation of the waves can be observed. Comparison of Figure 15(a) and Figure 15(b) prove that geometric damping leads to a rapid decay of the response amplitudes. According to Figure 15(b) the maximum peak velocities develop at the soil surface, because Rayleigh waves have the largest energy content. Furthermore, the faster propagating P-waves can be distinguished from the slower S-waves. According to the characteristics of P-waves in zones between compression and dilatation the velocities are zero.

For a layered elastoplastic subsoil composed of a layer of sandy silt with thickness of 1 m, which rests on sandy gravel, Figure 16 presents an overview of the velocity magnitude and the acceleration magnitude at time $t = 0.29$ s after the first compaction impact. It can be observed that in the layer with low stiffness the propagation velocity of the waves is considerably smaller than in the stiff halfspace. In the layer of sandy silt the dynamic response is much larger than in the sandy gravel. This can be attributed to diffraction, refraction, and reflection of the waves at the interface, and therefore reduced geometric damping.

ACKNOWLEDGMENTS

The Austrian Research Promotion Agency (FFG) has funded this research project. This support is gratefully acknowledged.

REFERENCES

[1] D. Adam, and I. Paulmichl. *Impact compactor – an innovative dynamic compaction device for soil improvement.* In: Proc. 8th International Geotechnical Conference (June 4-5, 2007, Slovak University of Technology, Bratislava, Slovakia), pp. 183-192, 2007.

[2] F.-J. Falkner, C. Adam, I. Paulmichl, D. Adam, and J. Fürpass. *Rapid impact compaction for middle-deep improvement of the ground – numerical and experimental investigation*. In: 14th Danube-European Conference on Geotechnical Engineering "From Research to Design in European Practice", June 2-4, 2010, Bratislava, Slovakia, CD-ROM paper, 10 pp., 2010.

[3] C. Adam, F.-J. Falkner, D. Adam, I. Paulmichl, and J. Fürpass. *Dynamische Bodenverdichtung mit dem Impulsverdichter* (*Dynamic soil compaction by the Rapid Impact Compactor*, in German). Project No. 815441/13026 – SCK/KUG, Final report for the Austrian Research Promotion Agency (FFG), 184 pp., 2010.

[4] A. Verruijt. *An introduction to soil dynamics*. Springer, Dordrecht, 2010.

[5] DIN 4150-1. *Vibrations in buildings - Part 1: Prediction of vibration parameters* (in German), June 2001.

[6] DIN 4150-1. *Vibrations in buildings - Part 2: Effects on persons in buildings* (in German), June 1999.

[7] ÖNORM S 9020. *Building vibrations; blasting vibrations and comparable immissions of impulse shape* (in German), August 1986.

[8] DIN 4150-3. *Vibration in buildings - Part 3: Effects on structures* (in German), February 1999.

[9] SN 640 312 a. *Vibrations-effects on buildings* (in German and French); April 1992.

[10] ÖNORM S 9010. *Mechanical vibrations-shocks, principles and evaluation of vibration quantities* (in German), February 1978.

[11] TERRA-MIX. Information from the website, www.terra-mix.com.

[12] HBM measurement. Information from the website of the manufacturer, www.hbm.com.

[13] SYSCOM instruments. Information from the website of the manufacturer, www.syscom.ch.

[14] DIN 45660-1. *Measurement of vibration immission - Part 1: Vibration meters - Requirements and tests* (in German), September 2010.

[15] ZIEGLER consulatants: Information from the website of the company, www.z-c.ch.